



Comparing regional transcript profiles from maize primary roots under well-watered and low water potential conditions

V. Poroyko¹, W. G. Spollen², L. G. Hejlek³, A. G. Hernandez⁴, M. E. LeNoble³, G. Davis³, H. T. Nguyen³, G. K. Springer², R. E. Sharp³ and H. J. Bohnert^{1,4,*}

¹ Department of Plant Biology and Department of Crop Sciences, University of Illinois at Urbana-Champaign, Urbana, IL 61801, USA

² Department of Computer Science, University of Missouri, Columbia, MO 65211, USA

³ Division of Plant Sciences, University of Missouri, Columbia, MO 65211-0001, USA

⁴ W. M. Keck Center for Comparative and Functional Genomics, University of Illinois at Urbana-Champaign, Urbana, IL 61801, USA

Received 12 March 2006; Accepted 14 July 2006

Abstract

Regionally distinct elongation responses to water stress in the maize primary root tip have been observed in the past. A genetic basis for such differential responses has been demonstrated. Normalized bar-coded cDNA libraries were generated for four regions of the root tip, 0–3 mm (R1), 3–7 mm (R2), 7–12 mm (R3), and 12–20 mm (R4) from the root apex, and transcript profiles for these regions were sampled. This permitted a correlation between transcript nature and regional location for 15 726 expressed sequence tags (ESTs) that, in approximately equal numbers, derived from three conditions of the root: water stress (water potential: –1.6 MPa) for 5 h and for 48 h, respectively, and well watered (5 h and 48 h combined). These normalized cDNA libraries provided 6553 unigenes. An analysis of the regional representation of transcripts showed that populations were largely unaffected by water stress in R1, correlating with the maintenance of elongation rates under water stress known for R1. In contrast, transcript profiles in regions 2 and 3 diverged in well-watered and water-stressed roots. In R1, transcripts for translation and cell cycle control were prevalent. R2 was characterized by transcripts for cell wall biogenesis and cytoskeleton

formation. R3 and R4 shared prevalent groups of transcripts responsible for defence mechanisms, ion transport, and biogenesis of secondary metabolites. Transcripts which were followed for 1, 6, and 48 h of water stress showed distinct region-specific changes in absolute expression and changes in regulated functions.

Key words: Maize root tip, normalized cDNA libraries, regional transcript profiles, unigene set, water deficit.

Introduction

The activity of the plant root apical meristem generates new cells whose subsequent lineages have been much studied genetically and developmentally (Benfey and Scheres, 2000; Beemster *et al.*, 2003). In the tip region, spatial and temporal patterning during sequential divisions generates the cells of the root cap and cells that undergo further divisions, expansion growth, and eventually differentiate into epidermis, cortex, endodermis/pericycle, vasculature, and vascular parenchyma of the primary root (Scheres and Heidstra, 1999; Casimiro *et al.*, 2003; Schiefelbein, 2003; Birnbaum and Benfey, 2004; Malamy, 2005). Processes that initiate cell division and expansion in the root tip have

* To whom correspondence should be addressed. E-mail: bohnerth@life.uiuc.edu

Abbreviations: EST, expressed sequence tag; ROS, reactive oxygen species; SAGE, serial analysis of gene expression; WA, water stressed; WW, well watered.

also been studied (Erickson and Sax, 1956; Macleod, 1991; Ishikawa and Evans, 1995; Baskin, 2000). Successive divisions, early isodiametric growth, and elongation growth have been integrated into models describing differentiation and expansion growth of the root tip (Sharp *et al.*, 1988; Baluška *et al.*, 1990; Ishiwaka *et al.*, 1991; Baskin, 2000; Dolan and Davies, 2004).

The importance of hormones, in particular, auxin and auxin transport regulation, has been shown for primary root elongation, gravity responses, as well as lateral root formation, and other hormones, for example, ethylene and abscisic acid (ABA), also play crucial roles in the adaptation of growth to external stimuli (Ishiwaka and Evans, 1993, 1995; Muday and Haworth, 1994; Rashotte *et al.*, 2000; Noh *et al.*, 2001; Sharp, 2002; Woll *et al.*, 2005). Quantitative analyses of root growth in *Arabidopsis* ecotypes have confirmed the existence, indicated much earlier, of the genetic basis for root elongation (O'Toole and Bland, 1987; Loudet *et al.*, 2005). The reactions of the root apical meristem and the elongation and differentiation processes are an important aspect of how plants respond to a variety of environmental factors that limit growth. Among those, drought is of particular interest, because of the importance of root growth maintenance or resumption in response to water deficits in an agricultural context.

Extensive study of the maize primary root system has been conducted by Sharp and co-workers (Sharp *et al.*, 1988, 2004; Spollen *et al.*, 2000; Sharp, 2002). As a result, four regions of the maize primary root tip have been identified based on their differential elongation rates under well-watered (WW) and water-stressed (WS) conditions. The spatial distinction of regions that showed cell expansion under both conditions from regions with expansion growth only in WW roots provided information to begin an analysis of transcriptional events that influenced root growth under water stress in a region-specific manner.

Microarray hybridizations allow for high-throughput monitoring of transcriptional activity of many genes. Until recently, such transcript profiling was limited to whole plants or organs. The presence of various cell types in such samples, each type with a distinct transcript composition, results in mRNA profiles and gene expression reports that show intensities averaged over all cells in the organ studied. As a consequence, specific profiles are masked, in particular those that characterize small populations of specialized cells. Novel approaches, such as cell ablation and laser dissection of tissues, provide ways to obtain specific profiles (Sessions *et al.*, 2000; Nakazono *et al.*, 2003; Klink *et al.*, 2005), replacing classical cell fractionation approaches that tend to alter the transcript profiles. In addition, a novel methodology is the use of transgenically provided fluorescent markers, expressed in different cell types, and cell sorting to generate cell type- and region-specific transcript profiles from the primary root of *Arabidopsis thaliana*. This approach facilitated definition

of a global transcript map of this organ, identified domains that correlated gene expression to cell differentiation, and defined regions of the root with patterns of gene expression indicating biosynthetic activity related to hormonal homeostasis (Birnbaum *et al.*, 2003).

In maize, the primary root elongation zone is particularly amenable to analysis as it extends further, compared with many other species, from the quiescent centre to the region where vascular differentiation begins. This structural feature was exploited to define the composition of the root transcriptome in a kinematic context. First, results have already been presented characterizing the number of genes that represent the maize root tip transcriptome based on a SAGE (serial analysis of gene expression) library and SAGE tags (Sharp *et al.*, 2004; Poroyko *et al.*, 2005). Here data are presented based on the analysis of normalized, bar-coded cDNA libraries and the distribution of transcripts and their associated functions in four regions of the maize primary root. In addition, transcript profiles of the four root regions that mirror the developmental gradient from the root meristem (region one) progressing to region 4, in which differentiation of the vasculature begins, were assessed in order better to define region-specific transcript populations. Finally, transcript populations were compared from root tip regions growing at different water potentials over a 48 h time-scale. Comparing transcript abundance in WW and WS conditions by quantitative reverse transcription-polymerase chain reaction (RT-PCR), the expression of a selected group of genes indicated functions associated with the progression of water stress and extraordinarily large spatial divergence in gene expression.

Materials and methods

Generation of material for cDNA library constructions

Dark-grown maize seedlings (cv. FR697) with primary roots 12–20 mm in length were transplanted to high water potential (−0.03 MPa) or low water potential (−1.6 MPa) vermiculite, and harvested 5 h and 48 h after transplanting. Approximately 1000 roots were used for each of the water-stressed cDNA libraries, zmrws05 and zmrws48, respectively, while 500 roots were harvested at each time (5 h and 48 h, respectively) and combined to generate the well-watered cDNA library zmrww (WW00). For details of growth conditions, see Sharp *et al.* (1988) with nutrient modifications as in Spollen *et al.* (2000). The apical 20 mm of each root was sectioned into four regions (distances are from the junction of the root apex and root cap): region 1 (R1), 0–3 mm plus the root cap; region 2 (R2), 3–7 mm; region 3 (R3), 7–12 mm; region 4 (R4), 12–20 mm. For quantitative PCR analyses, the same root regions were harvested at 1, 6, and 48 h after transplanting to high or low water potential conditions.

Generation of normalized cDNA libraries

Primary library construction was performed by an established protocol (Soares and De Fatima Bonaldo, 1997). Total RNA was extracted by the 'hot phenol' method, which effectively eliminated carbohydrate abundantly present in root tips (Pawlowski *et al.*, 1997). The integrity of the RNA was verified by denaturing agarose gels and spectrophotometry (ratio $A_{260\text{nm}}/A_{280\text{nm}}$). Poly(A)⁺ mRNA

was isolated twice from total RNA using the Oligotex Direct mRNA kit (Qiagen, Valencia, CA, USA). First-strand cDNA synthesis was conducted on each pool using unique *NotI*/oligo(dT) primers that differed by the inclusion of unique 5 bp DNA sequences embedded between the *NotI* cloning site and (dT)₁₈. The modified oligo(dT) primers were as follows: R1, (NotI)ACGCA18(T); R2, (NotI)ACCGA18(T); R3, (NotI)TCGCA18(T); and R4, (NotI)TCCGA18(T). They served as bar-codes for later recognition of their region of origin.

The resulting double-stranded cDNAs were size selected (>450 bp) and cDNA products for different regions of the same library were pooled in equivalent proportions for subsequent cloning. Size-selected cDNA mixtures were adapted with *EcoRI* adaptors at both ends, and then digested with *NotI*. The cDNA was directionally cloned into *EcoRI*–*NotI*-digested pBS II SK(+) phagemid vector (Stratagene, La Jolla, CA, USA) and electroporated into *Escherichia coli* DH10B. The total number of white colony-forming units (cfu) in the primary libraries before amplification was as follows: zmrws05, 3.37×10^6 ; zmrws48, 4.87×10^6 ; zmrww00, 3×10^6 . The background of empty clones was <1%. Inserts ranged from ~0.5 to >2.5 kb, as determined by PCR of 96 clones from each library (not shown). After transformation, bacterial cells were inoculated into 250 ml of LB medium and grown overnight. Plasmid DNAs were isolated by using Qiagen QIAfilter Plasmid Maxi Kit (Qiagen).

Plasmid DNA from the primary libraries then was converted to single-stranded circles by Gene II digestion and exonuclease III treatment. A 4 µl aliquot of each library was used as a template for PCR amplification (four reactions per library, 1 µl per reaction) using the T7 and T3 priming sites flanking the cloned cDNA inserts. The purified PCR products, representing the entire cDNA population cloned in each library, were used as a driver for normalization. Hybridization between the single-stranded library and the PCR products was carried out for 44 h at 30 °C. Non-hybridized single-stranded DNA was separated from hybridized DNA rendered partially double-stranded by HAP hybridization, converted into double-stranded DNA with Sequenase using the M13 (–21) primer, and electroporated into DH10B.

DNA sequencing

The normalized libraries were plated on agar and colonies were robotically picked with a Genetix Q-pix robot and racked as glycerol stocks in 384-well plates. After overnight growth of the glycerol stocks, bacteria were inoculated into 96-well deep cultures with LB medium and carbenicillin (100 mg ml^{–1}), and grown overnight. Plasmid DNA was purified from the bacterial cultures using the Qiagen 8000 and Qiagen 9600 BioRobots. Sequencing reactions were performed using BigDye terminator chemistry (Applied Biosystems, Foster City, CA, USA), using the standard primer M13 reverse for –48. Sequencing of the 3' ends of the clones was performed on the ABI 3730xl capillary system. All 384- and 96-well format plates were bar-coded and a laboratory information management system (HTLims) was used to track sample flow.

Bioinformatics tools and EST analysis

Base calling was performed by Phred (Ewing *et al.*, 1998). Bases with a Phred score ≥ 20 were accepted. Expressed sequence tag (EST) sequences were assembled using tl-cluster (<http://genome.uiowa.edu/pubsoft/software.html>). Sequence similarity analyses were performed using BLAST software (Altschul *et al.*, 1990). Several BLAST databases were used for annotation: NCBI UniGene Build #40 *Zea mays* (non-redundant protein database NCBI), and the database of 'Clusters of orthologous groups for eukaryotic complete genomes'. The cut-off value for BLASTX and BLASTN was set as lower than 10^{-5} , but most identifications were reported at much lower e-values. The list of *A. thaliana* genes involved in different biochemical pathways was taken from the TAIR website ([\[arabidopsis.org/\]\(http://arabidopsis.org/\)\). Similarity clustering was done by Spotfire DecisionSite 7.2 using the clustering method, WPGMA \(weighted average\); similarity measure, Euclidean distance; ordering function, average value.](http://</p>
</div>
<div data-bbox=)

To detect conserved functional domains, orthologous genes for completely sequenced genomes, based on an analysis of seven complete eukaryotic genomes, were used as templates: *A. thaliana*, *Caenorhabditis elegans*, *Drosophila melanogaster*, *Homo sapiens*, *Saccharomyces cerevisiae*, *Schizosaccharomyces pombe*, and *Encephalitozoon cuniculi* (Tatusov *et al.*, 2001). Hits of identity in functional domains were taken as a description for each unigene, while sequences lacking hits, and orphans without association to a cluster after BLASTX were considered in category [S] (KOG nomenclature; function unknown). The overall functional diversity of a region was then determined as the percentage of sequences in a category in relation to all sequences in this region (for the complete data set, see: Supplementary Table 1 available at JXB online).

Real-time PCR

Real-time PCR primers (Supplementary Table 3 available at JXB online) were designed to meet these criteria: T_m 600 °C and PCR product length 115 bp. For primer design, Gene Runner v3.5 and several homemade Perl scripts were used. Primers were examined *in silico* to determine possible competitive annealing with unspecific maize transcripts by BLASTN search versus the NCBI Maize Unigene Set (Build #40). All sequences used for primer design (parental sequences) were tested by BLASTN against the Maize Unigene Set (Build #40). The corresponding pairs 'parental sequence to primer' and 'parental sequence to unigene' were established. Primers were considered unspecific if a hit with a unigene differed from that previously established as a top hit for 'parental sequence', and the annealing temperature for the region of homology was >500 °C. Annealing temperatures were determined according to the nearest-neighbour thermodynamic value method (Breslauer *et al.*, 1986).

Primers were synthesized by Integrated DNA Technologies Inc. (Coralville, IA, USA), and tested as described (User Bulletin #2 for ABI PRISM 7700 Sequence Detection System). Primer pairs that passed all tests were assembled in 96-well master plates with the final concentration of each primer at 0.5 µM, and 8 µl of mixture were transferred to 384-well plates in four replicates and vacuum dried. The 384-well plates with dried primers were used for quantitative PCR amplification.

Total RNA was isolated from 12 samples (segments 1–4, time-course for each segment: 1, 6, and 48 h), treated with DNase ('DNA-free', Ambion, Austin, TX, USA), and the concentration and quality were examined. Then 0.5 µg of total RNA from each sample was used in reverse transcription reactions using Superscript III (Invitrogen, Carlsbad, CA, USA) according to the manufacturer's instructions. The reaction mixture was then diluted 20-fold and used as a template for real-time PCR. The reaction composition combined 5 µl of SYBR Green PCR master mix, 4.6 µl of water, and 0.4 µl of template. Real-time PCR data were used for direct $\Delta\Delta Ct$ analysis as described in the User Bulletin #2 for ABI PRISM 7700 Sequence Detection System. All $\Delta\Delta Ct$ -values were normalized relative to the amount of transcripts for actin-3 (gi|21206665) present in each segment, while the amount of this control transcript itself varied between segments. Transcription levels were calculated according to $2^{\Delta Ct} \times 100\%$, where $\Delta Ct = Ct_{actin} - Ct_{gene}$ of interest with the expression level of actin taken as 100%.

Results and discussion

Transcript profiles are an indispensable requisite for understanding the functioning of cells, organs, and the whole

plant. While such profiles will not predict or precisely identify the complement of proteins and protein activities active in cells or organs, transcript nature and abundance identify the status of the signalling and response machineries that describe homeostatic conditions at the time of tissue sampling. Increasingly, such profiles are collected in the form of microarray hybridizations of mRNAs (cDNAs) against printed or synthesized segments of genes in high-throughput fashion (Birbaum *et al.*, 2003). Also, ESTs and SAGE tag collections can be used to establish which transcripts are present in a tissue (Blancaflor *et al.*, 1999; Gowda *et al.*, 2004; Bruggman *et al.*, 2005). Based on the large number of tags that can be obtained, SAGE tends to provide even greater confidence about which genes are expressed in a sample. When the sample size of sequenced cDNAs or SAGE tags is large enough, these tools can provide an even more precise measurement of transcript abundance than microarrays.

However, in each case, when RNA from an entire plant, from leaves, roots, or flowers provides the starting material, an averaged representation of the transcript profile results that disregards the contribution of specialized cells or developmental gradient within a tissue. The isolation of cells by various methods, including physical separation from a tissue by, for example, centrifugation, cell sorting, or ablation techniques, can provide the material for more detailed characterizations of the expressed transcriptome (Nakazono *et al.*, 2003; Klink *et al.*, 2005). Based on the detailed physiological and, for the expansin family, molecular analyses on the behaviour of the maize root tip under water deficit conditions (Sharp *et al.*, 1988; Spollen *et al.*, 2000; Wu *et al.*, 2001), transcripts were sampled from regions of the root for which precise measurements of growth are known.

ESTs and their functional identities in different regions of the maize root tip

Figure 1 presents in schematic form the spatial distribution of displacement velocity in the maize primary root tip under WW and WS conditions; local elongation rates are obtained from the derivative of velocity with respect to position. The original displacement velocity data for cv. FR697, used in this study, were reported by Sharp *et al.* (2004). Similarly to previous analyses (Sharp *et al.*, 1988; Liang *et al.*, 1997), four regions with distinctly different elongation characteristics may be discerned. In region 1, displacement velocities are the same in WW and WS roots, supported by the continuous generation and expansion of new cells. Under WW conditions, maximal elongation rates occur in region 2, while the elongation rate declines in region 3 and terminates in region 4. Under WS conditions, the decline in elongation rate is already observed in region 2 and terminates in region 3. Finally, differentiation of vascular tissues starts in the distal parts of region 4 (WW).

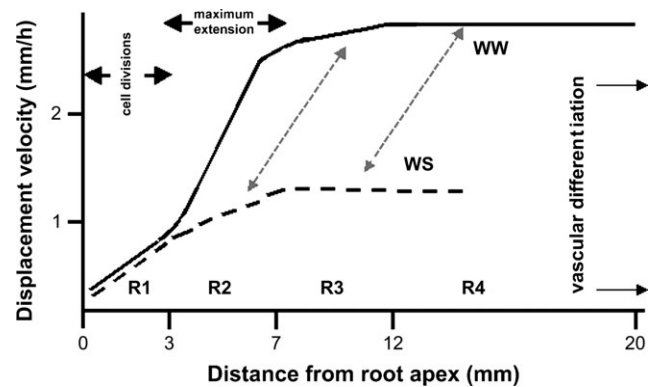


Fig. 1. Schematic representation of the spatial distribution of the displacement velocity rate in the maize primary root tip. The original data for cv. FR697, used in this study, were reported in Sharp *et al.* (2004), and were calculated from root elongation rates and cortical cell length profiles at 48 h after transplanting to well-watered (water potential of -0.03 MPa, solid line, WW) or water-stressed (water potential of -1.6 MPa, broken line, WS) conditions. Regions 1–4 are indicated.

Primary roots from three conditions (WW 5 h and 48 h combined; WS 5 h; and WS 48 h) were cut into the four root regions (Fig. 1; R1 also included the root cap), and RNAs were isolated. Transcripts from each region were provided with a five-nucleotide bar-code adjacent to the poly(A) tail for segment identification and converted into primary cDNA libraries. For each condition, the bar-coded transcripts for each of the four regions were combined, and normalized cDNA libraries were generated. DNA sequencing from the cDNA 3' ends of 18 048 cDNA clones was carried out. This included 5760 clones from the library WW00, which included RNA from root segments collected at 5 h and 48 h to maintain the same developmental age compared with root segments harvested under water deficit conditions. For each of the libraries WS05 and WS48, 6144 clones were determined. Of these, 15 726 (87.1%) resulted in high-quality EST sequences that have been deposited in GenBank, and used for further analysis: bar-code extraction, contig assembly, and homology searches.

Bar-codes were unequivocally identified in 13 728 ESTs (87.2%). Their distribution across the three root libraries is shown in Table 1. At this stage, a significant under-representation of unigene clusters became apparent for transcripts from R2 at 5 h and 48 h under water stress. Using 'tl-cluster' (<http://genome.uiowa.edu/pubsoft/software.html>), the 15 726 ESTs were assembled into 6553 unigene clusters and each contig annotated by BLASTX against the non-redundant protein database at NCBI. Similarity clustering by Spotfire DecisionSite 7.2, in terms of the abundance and function of each transcript, indicated that all R1 segments, whether derived from WW or WS conditions, were most similar (Fig. 2). The profiles in other regions diverged such that transcripts found in R2/R3 (WW) were similar to the profile in R2 (WS05), while the profile for R4 (WW) mirrored WS48 R2 as well as the regions

Table 1. Numbers of ESTs and unique gene clusters in different regions of the maize root tip

| Library | R1 | | R2 | | R3 | | R4 | | Region unknown ^a | | Total ESTs |
|---------|------|----------|------|------------------|------|----------|------|----------|-----------------------------|----------|------------|
| | ESTs | Clusters | ESTs | Clusters | ESTs | Clusters | ESTs | Clusters | ESTs | Clusters | |
| ww00 | 1337 | 976 | 1166 | 887 | 739 | 608 | 738 | 618 | 918 | 679 | 4898 |
| ws05 | 1540 | 1069 | 342 | 305 ^b | 1461 | 1126 | 1368 | 1065 | 611 | 441 | 5322 |
| ws48 | 663 | 531 | 375 | 329 ^b | 2833 | 2010 | 1166 | 944 | 469 | 362 | 5506 |

^a Bar-code not identified or uncertain.

^b The low number of clusters in WS05-R2 and WS48-R2 is interpreted as an indication of reduced transcription in these regions, while the nature of the transcripts showed significant overlap with the profiles in R1 and R3, respectively.

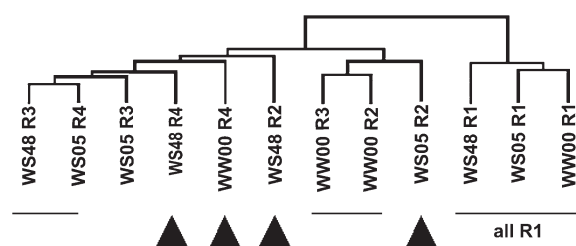


Fig. 2. Clustering of transcripts in four regions of the maize primary root under well-watered and water-stressed conditions. Cluster analysis (Spotfire DecisionSite 7.2) using functional complexity of unigenes reveals the degree of similarity between regions and treatment conditions. Underlined are segment profiles with considerable similarity, i.e. transcripts in all segments R1, irrespective of the conditions, are most similar to each other and different from all other regions. Triangles indicate regions with distinctly different transcript composition in terms of the functional categories. A clustering result reported previously (Sharp *et al.*, 2004) had considered similarity scores according to EST abundance.

R3/4 under water stress conditions (Fig. 2). It appears that transcripts found in WS roots are to some degree closer to the root apex than in WW roots (Fig. 2). The regions R2 with the largest difference in elongation rate between WW and WS conditions showed most divergent transcript compositions in terms of functional categories. All ESTs have been deposited at the NCBI database and are available: <http://rootgenomics.missouri.edu/prgc/index.html>.

Functional annotation

The 6553 unique transcripts that could be categorized and identified by region-specific bar-codes were clustered according to functional categories as defined by KOG (Babenko and Krylov, 2004). The inclusion in functional categories and frequency of transcripts in any category, represented by a colour gradient, is shown in Fig. 3. The highest similarity among treatments in the nature of transcripts was seen for R1. This could suggest that the root meristem might be largely insulated from the water deficit treatment. In absolute numbers, transcripts in four functional categories were most frequent and quite uniformly represented in all regions of the root tip. These categories identified 'Post-translational modifications', 'Translation', 'Energy production', and 'Signal transduction' (Fig. 3).

The pattern that emerged showed relationships between region, condition, and duration of water stress (Fig. 3). Other

functional categories expressing the same pattern to some degree, albeit with smaller absolute numbers, were 'Cell cycle control/cell division', 'Chromatin structure', 'Replication', and 'RNA metabolism'. Differences existed in that, for example, cell cycle-specific transcripts persisted in R2 in the WW root, although not in WS conditions, declined in R3, and increased again in R4 (Fig. 4B). Taken together, these four categories indicated cell proliferation functions that are consistent with cytological parameters, while the resumption of transcripts in functions in cell cycle and chromatin structure in R4 of the WW root provided an indication of cell divisions resuming as vascular differentiation begins. The absence of transcripts in this function indicated a delay in the developmental programme in R4 of WS roots. Cell wall biosynthesis and modification, and cytoskeleton functions were more prevalent in R2, relative to R1 (Fig. 4C, D). Defence-related transcripts displayed a different pattern characterized by a few transcripts in R1 and steady increases in R2–R4 (Fig. 4E); the increase was less in R4 of the roots stressed for 48 h, possibly indicating terminal damage in these long-term severely stressed roots. A similar abundance pattern is observed for other categories, with transcripts in the category 'Ion and water transport' representing a prime example (Fig. 4F) that documents the development of the maturing root into an organ with a primary function in nutrient acquisition. Yet another dynamic of transcript presence is shown by sequences identified in the category 'Secondary metabolism' (Fig. 4G). While the number of transcripts is low in R1 under all conditions, in all subsequent regions these transcripts increased ~3-fold irrespective of growth or stress conditions.

In the three root cDNA libraries, 11 unigene clusters (33 ESTs) were annotated as expansins (ST 2a). These clusters were not evenly distributed within the library segments. R1 was devoid of expansin unigenes, while R2, R3, and R4 were relatively enriched in expansin transcripts (see also Wu *et al.*, 2001). In R4, five expansin transcript contigs were present. A similar distribution was found for transcripts encoding major intrinsic proteins [aquaporin (AQPs)], a group of 10 unigenes totalling 62 ESTs (ST 2b). Transcripts for vacuolar (H⁺)-ATPases (ST 2c) identified 14 unigene clusters (83 ESTs). The regions WW00-R1 and WS05-R1 (5 h stress) contained the highest number of unigenes for vacuolar (H⁺)-ATPase subunits,

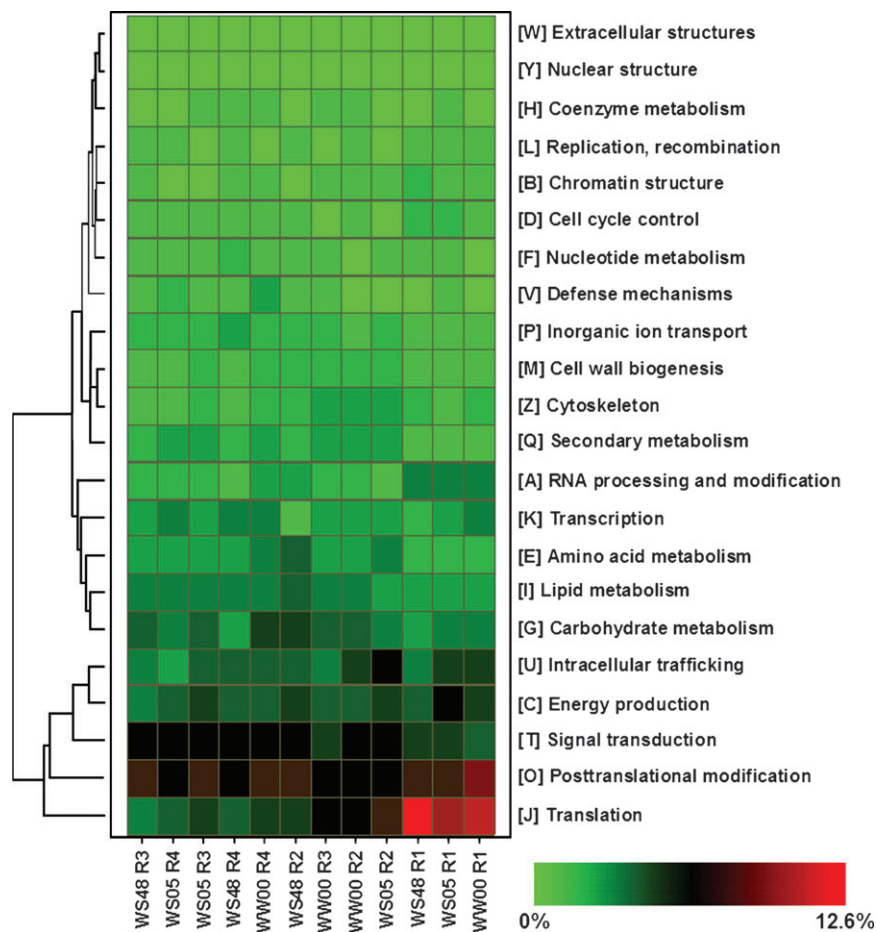


Fig. 3. Transcript clusters in different regions of well-watered and water-stressed roots sorted by functional categories. The abundance of transcripts per region in a functional category is indicated by colour intensity.

seven and 10, respectively. After 48 h of stress, this number declined significantly in R1 while the higher numbers had shifted to R3. Also, 20 unigenes (46 ESTs) related to auxin responses were detected (ST 2d). These transcripts were concentrated in R3 and R4 in all three cDNA libraries. No cDNA for this function was present in R1, and after 48 h of water stress no auxin-related cDNA was detected in R4. In WW roots, maximum numbers were found in R4, and even higher frequencies occurred in segments R2 and R3 of roots stressed for 48 h. The distribution in the cDNA library zmrws05 showed an intermediate distribution, with some cDNAs detected in R1. Water stress led to the induction of auxin-responsive and auxin biosynthesis-related genes in a regionally distinct pattern.

A similarly different distribution was found for transcripts associated with the biosynthesis of jasmonates and jasmonate signalling components (Table 2). Of the 47 unigene transcripts for these functions, 162 ESTs in total, a larger number were found in R2 of the WW root, while under water deficit a high number of unigene transcripts was obtained in segments R3 and R4, again highlighting the altered developmental progression of the root.

Quantitative PCR analyses

Results that emerged from the analysis of transcripts in functional categories were verified and further analysed by a time-course analysis of transcript changes after 1, 6, and 48 h of water stress (Fig. 5). The functional clustering had already revealed general patterns of transcript expression that could be expected, and confirmed information obtained from kinematic analyses, cell biology, and physiology. However, how these patterns changed within short spatial boundaries indicated expression complexities that were, in part at least, unexpected and significant. In further analyses, an additional level of precision was sought by analysing selected transcripts that exhibit regionally distinct functions in more detail using quantitative, real-time PCR analyses. Values are expressed as a percentage of transcript compared with the amount of an actin gene (actin-3, gi|21206665) measured at the same times in regions 1–4 under WW conditions (Fig. 5).

Transcript changes in reactive oxygen species (ROS)-scavenging activities, exemplified by the maize Cat3 gene (gi|168436), are shown in Fig. 5A. Catalases, which are ubiquitous, have been shown to be induced under heavy

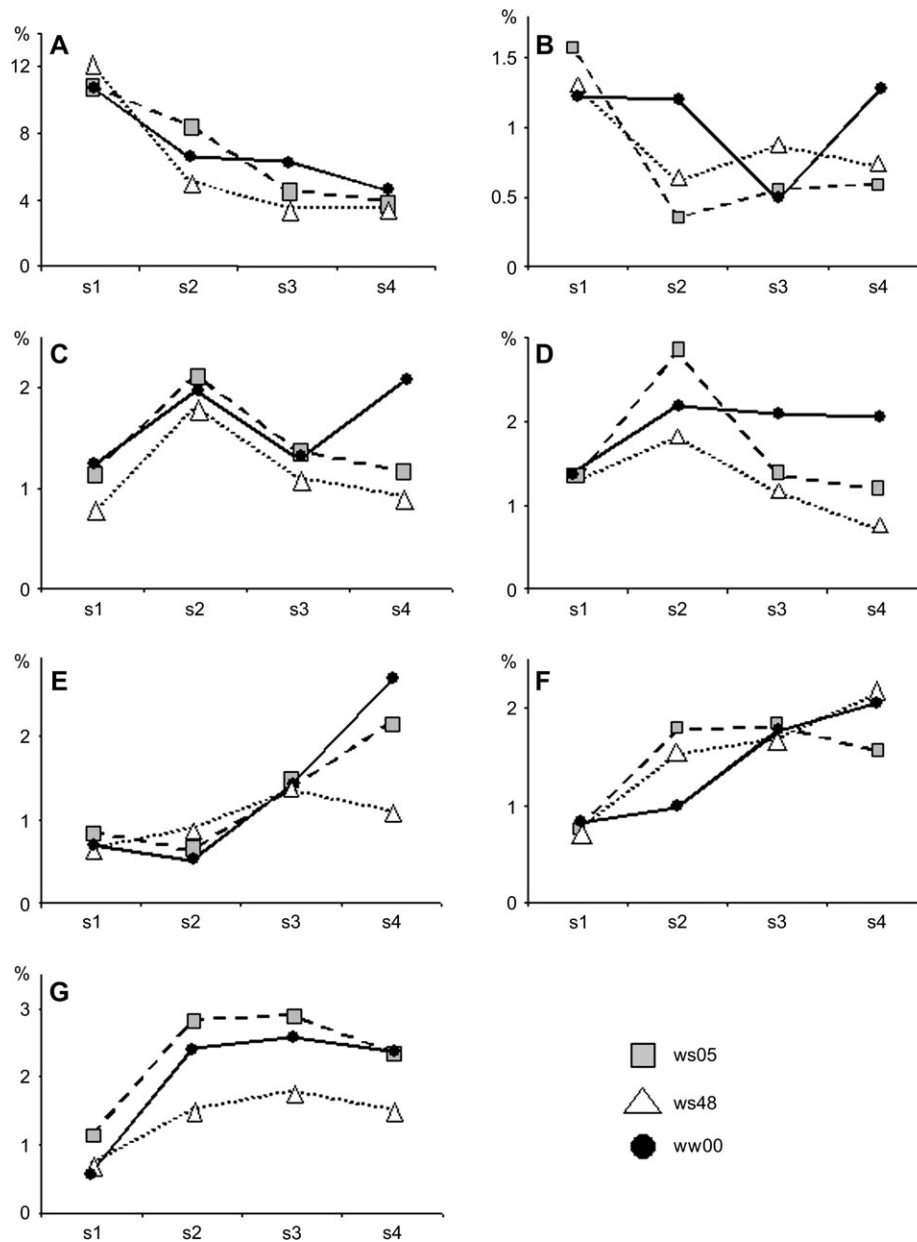


Fig. 4. Quantitative analysis of transcripts for selected functions. Amounts of contigs are shown as a percentage of all transcripts in the region. (A) Translation, ribosome structure, and biogenesis; (B) cell cycle-related; (C) cell wall/membrane biogenesis; (D) cytoskeleton; (E) defence-related; (F) inorganic ion and water transport/metabolism; (G) related to secondary metabolism. Circles, library zmrww00 (well watered); squares, library zmrws05 (water stress, 5 h); triangles, library zmrws48 (water stress, 48 h).

metal stress conditions (Boscolo *et al.*, 2003). Generally, under WW conditions Cat3 constituted a rare transcript in R1, and water stress elevated its abundance only minimally at any of the three time points. Taking into account the different scales for transcript abundance, catalase transcripts remained low in R2 and R3 in WW roots, but increased in R4. While Cat3 transcripts in R1 changed only marginally after 1 h of water stress, they were up-regulated at later time points in all four regions, 2–4-fold at 6 h and >20-fold at 48 h relative to WW conditions (Fig. 5A). Cat3 mRNA levels have been reported from

developing maize seedlings before (Redinbaugh *et al.*, 1990). High levels of the Cat3 transcript were present in the root, epicotyl, and leaf, with a positive correlation between the accumulation of transcript and catalase isozyme. The result from the time-course analysis seems to indicate an increasing necessity for ROS scavenging as the water deficit stress increased, while the complexity of ROS-scavenging activities in R1 of WW conditions appears to represent the homeostatic equilibrium. As a group, ROS-scavenging enzymes (ST-2) included 30 unigene clusters (145 ESTs). R1 of WW roots revealed the highest number

Table 2. Root tip unigenes associated with phytohormone metabolism and signalling

Values in parentheses are the percentage of unigenes in the category in each region.

| Library | R1 | R2 | R3 | R4 |
|-------------|-----------|------------|------------|------------|
| Gibberellin | | | | |
| ww00 | 2 (0.21%) | 5 (0.56%) | 4 (0.66%) | 1 (0.16%) |
| ws05 | 2 (0.19%) | 1 (0.33%) | 6 (0.53%) | 4 (0.38%) |
| ws48 | 0 (0%) | 1 (0.30%) | 6 (0.30%) | 4 (0.42%) |
| Auxin | | | | |
| ww00 | 3 (0.31%) | 6 (0.68%) | 4 (0.66%) | 10 (1.6%) |
| ws05 | 6 (0.56%) | 2 (0.66%) | 20 (1.79%) | 10 (0.90%) |
| ws48 | 2 (0.38%) | 3 (0.91%) | 17 (0.85%) | 11 (1.18%) |
| Jasmonate | | | | |
| ww00 | 4 (0.41%) | 12 (1.35%) | 5 (0.82%) | 6 (0.97%) |
| ws05 | 6 (0.56%) | 1 (0.33%) | 11 (0.98%) | 8 (0.75%) |
| ws48 | 3 (0.57%) | 3 (0.91%) | 13 (0.65%) | 8 (0.85%) |

of unigenes for ROS-scavenging enzymes (eight). Water stress changed the unigene number, type, and distribution under water stress conditions: 14 and 10 ROS unigenes, respectively, were present in R3 after 5 h and 48 h of water stress.

On a different, much higher, mRNA abundance scale, the behaviour of a MIP transcript, the water channel PIP1-2 (gi|4768910), mirrored the expression of Cat3 early during water stress. The regionally distinct transcript abundance for this AQP has previously been determined using northern-type analyses (Hukin *et al.*, 2002). The present results, determined by unigene counts and real-time RT-PCR, correlate well with these previous findings. Water stress enhanced the amount of this transcript by a factor of ~2 (Fig. 5). Variations on the theme were seen when transcripts of a plasma membrane proton-ATPase (gi|758354) or an alternative oxidase (gi|2811175) were chosen. The ATPase transcripts were more abundant in R4, and a decline after 48 h in both WW and WS conditions was observed; water stress did not significantly affect the amount of this transcript. Finally, transcripts for the alternative oxidase were reduced by short-term water stress, but increased substantially after 48 h relative to WW conditions.

By generating cDNA libraries from four regions of the root tip, it was possible to detect >6500 expressed genes. Spatial resolution and the distribution of transcripts of a different nature highlight expression profiles and changes that cannot be obtained by an analysis of entire organs. A previous analysis (Birnbaum *et al.*, 2003) had used cell-specific promoters driving the expression of reporter proteins that could then be used to isolate specific cell populations by sorting. The identification and comparison of cell type-specific and age-specific (in terms of distance from the meristem) transcripts in the *Arabidopsis* root tip represented an excellent overview of regionally distinct, developmentally programmed gene expression. The present analysis, representing a developmental gradient along the

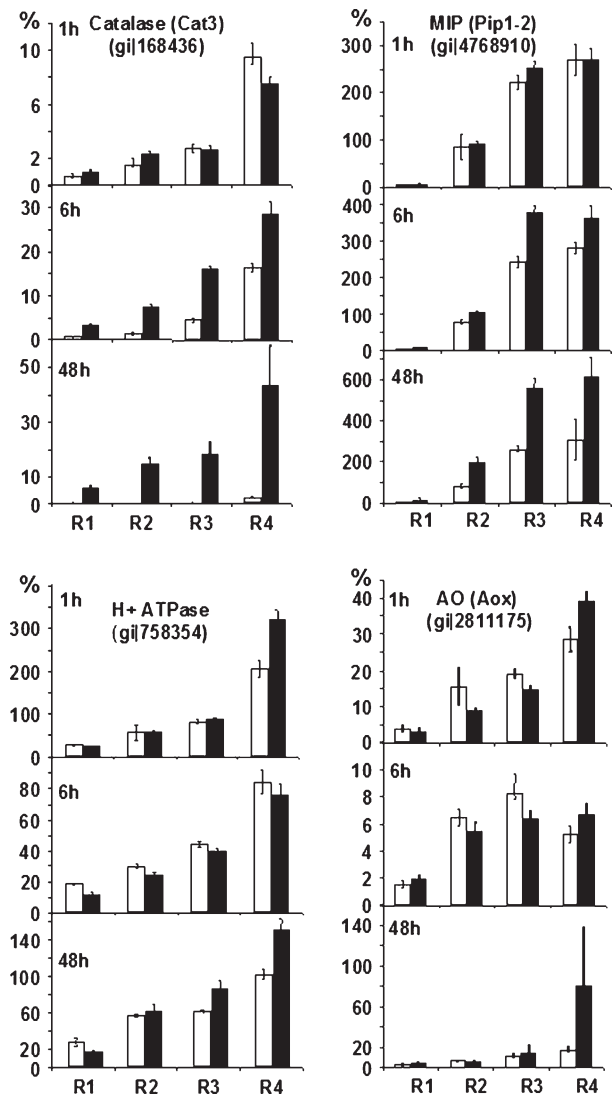


Fig. 5. Amounts and changes during water stress of selected transcripts. Amounts determined by quantitative RT-PCR are expressed as the percentage of transcript in relation to the amount of actin (Act-3, gi|21206665). White bars, well-watered conditions at 1, 6, and 48 h after transplanting. Black bars, water-stressed conditions at 1, 6, and 48 h after transplanting. (A) Catalase (*Z. mays*, gi|168436); (B) plasma membrane MIP protein [pip1-2 (gi|4768910)]; (C) H⁺-ATPase [*Z. mays* (gi|758354)]; (D) alternative oxidase [Aox (gi|2811175)].

maize root tip, now adds the physiological dimension of water stress. A number of correlations exist between the dicot and monocot root tip expression profiles under unstressed growth conditions. The correlation is strong with respect to the abundance of transcripts in particular categories in certain regions, for example, post-translational modifications, translation, and basic metabolism. Birnbaum *et al.* (2003) also defined regions in the stele and cortex at different distances from the meristem that were enriched for transcripts specifying hormonal functions. With respect to transcripts for gibberellin, auxin, and jasmonate biosynthesis genes, Birnbaum *et al.* (2003) defined a region putatively involved in auxin biosynthesis corresponding to R4

in our study. Likewise, the authors placed genes for jasmonate biosynthesis in the cortex, and genes involved in gibberellin biosynthesis in the stele in a region of the *Arabidopsis* root that would correspond to R2 in the present study. Unigenes for the three pathways in the maize WW primary root were detected: 44 transcripts for auxin biosynthesis and auxin-related genes, 27 for gibberellin-related functions, and 47 for jasmonate biosynthesis and signalling. The transcripts were present in all regions, but the highest numbers (and percentage relative to all unigenes in a region) were found in R3/4 for auxin-related functions, in R2/3/4 for jasmonates, and in R2/3 for gibberellin-related function (Table 2).

A similar approach to defining genes active in the elongation zone of the maize primary root has been reported (Bassani *et al.*, 2004). Using suppression subtractive hybridization, and northern-type and *in situ* hybridizations, 150 non-redundant transcripts were documented in regions of the root tip that coincided with the regions used in the present study. The cDNA libraries included these transcripts. As one example, Bassani *et al.* (2004) observed the over-representation of a vacuolar ATPase transcript in the region of accelerating elongation in WW maize roots and in roots under moderate water stress (-0.5 MPa). In *Arabidopsis* roots, similar expression in the elongation region was observed by Padmanaban *et al.* (2004) using β -glucuronidase (GUS) expression under the control of a vacuolar H^+ -ATPase promoter. In addition, Li *et al.* (2005) correlated expression of the vacuolar H^+ -ATPase in roots, apart from its function in maintaining vacuolar pH, with auxin transport and auxin-dependent development and cell division. The present study showed the highest number of unigenes for vacuolar (H^+)-ATPase subunits in R1 under WW conditions as well as after 5 h of water stress.

Conclusions

The maize primary root system is ideally suited for a high-throughput genomics-type analysis of the transcript complement present in regions that have been physiologically characterized under WW conditions by their functions in cell divisions and the onset of elongation (R1), maximum elongation rate (R2), deceleration of elongation (R3), and growth cessation and maturation (R4). Of further advantage is that these regions show distinctly different responses of elongation rate to water stress (Fig. 1). An analysis of the root tip transcriptome by SAGE documented the presence of almost 16 000 different transcripts, while the analysis and extrapolation of SAGE tags that are found in single copy (and thus excluded from the transcript count) suggest that at least 23 000 genes are transcribed in the maize root (Poroyko *et al.*, 2005). Additional information with respect to the responses to water deficit in different regions of

the primary root and the complexity of the root transcriptome is expected from microarray-based transcript profiling (K Chen, WG Spollen, RESharp, HT Nguyen, unpublished data).

The analysis of >6500 unigenes and their distribution in different regions of the primary root tip showed a distribution of transcripts in different categories that was partly expected, such as the large amount of transcripts for functions in cell cycle, cell division, and chromatin structure that were present in R1, which includes the quiescent centre. In addition, functions in cell expansion, cell wall biosynthesis, cell maturation, and hormone biosynthesis could be assigned to particular regions. However, a novel and unexpected finding was the wide range of transcript steady-state levels in different regions. Many transcripts were detected with a >10-fold different expression intensity in cells separated by a short distance along the root tip.

Under conditions of water stress, the transcript profiles changed in nature and location, in particular in R2. In contrast, R1 maintained to a large degree the profile that existed under WW conditions, and this region, with small cells largely devoid of a central vacuole, appeared to experience or sense less or no water deficit when taking into account transcripts that are typically associated with water stress conditions. In general, however, the cDNA profiles under water stress revealed a regional shift in transcripts in functional categories; transcripts found in R2 in WW cDNA libraries showed lower representation in segments R2 under WS conditions. The profiles emerging from WS-R2 and WS-R3 segments seem to represent and include a mixture of two programmes: earlier maturation, i.e. appearing earlier than in the WW root, and delayed development, showing functions that appear later than in the WW root. Considering these changes, we suggest that water stress sensing and response may be a function of R2 in which the jasmonic acid biosynthesis and signalling pathway transcripts appear to be more concentrated than in other regions. Determining the extent to which transcript profiles that record the influence of developmental and environmental changes on hormonal homeostasis are transferred into changes at the protein level will be the challenge of the future (Zhu *et al.*, 2006).

Supplementary material

Supplementary data can be found at JXB online.

Acknowledgements

We thank Vladimir Calugaru for help in data analysis and Perl programming. Additional materials are deposited at a project homepage, <http://rootgenomics.missouri.edu/prgc/index.html>. Our work is supported by a grant from the US National Science Foundation,

plant genome program (DBI-0211842), and by University of Missouri and University of Illinois internal support.

References

- Altschul SF, Gish W, Miller W, Myers EW, Lipman DJ. 1990. Basic local alignment search tool. *Journal of Molecular Biology* **215**, 403–410.
- Babenko VN, Krylov DM. 2004. Comparative analysis of complete genomes reveals gene loss, acquisition and acceleration of evolutionary rates in Metazoa, suggests a prevalence of evolution via gene acquisition and indicates that the evolutionary rates in animals tend to be conserved. *Nucleic Acids Research* **32**, 5029–5035.
- Baluška F, Kubica Š, Hauskrecht M. 1990. Postmitotic isodiametric cell growth in the maize root apex. *Planta* **181**, 269–274.
- Baskin TI. 2000. On the constancy of cell division rate in the root meristem. *Plant Molecular Biology* **43**, 545–554.
- Bassani M, Neumann PM, Gepstein S. 2004. Differential expression profiles of growth-related genes in the elongation zone of maize primary roots. *Plant Molecular Biology* **56**, 367–380.
- Beemster GTS, Fiorani F, Inzé D. 2003. Cell cycle: the key to plant growth control? *Trends in Plant Science* **8**, 154–158.
- Benfey PN, Scheres B. 2000. Root development. *Current Biology* **10**, R813–R815.
- Birnbaum K, Benfey PN. 2004. Network building: transcriptional circuits in the root. *Current Opinion in Plant Biology* **7**, 582–588.
- Birnbaum K, Shasha DE, Wang JY, Jung JW, Lambert GM, Galbraith DW, Benfey PN. 2003. A gene expression map of the *Arabidopsis* root. *Science* **302**, 1956–1960.
- Blancaflor EB, Fasano JM, Gilroy S. 1999. Laser ablation of root cap cells: implications for models of graviperception. *Advances in Space Research* **24**, 731–738.
- Boscolo PR, Menossi M, Jorge RA. 2003. Aluminum-induced oxidative stress in maize. *Phytochemistry* **62**, 181–189.
- Breslauer KJ, Frank R, Blocker H, Marky LA. 1986. Predicting DNA duplex stability from the base sequence. *Proceedings of the National Academy of Sciences, USA* **83**, 3746–3750.
- Bruggmann R, Abderhalden O, Reymond P, Dudler R. 2005. Analysis of epidermis- and mesophyll-specific transcript accumulation in powdery mildew-inoculated wheat leaves. *Plant Molecular Biology* **58**, 247–267.
- Casimiro I, Beeckman T, Graham N, Bhalerao R, Zhang H, Casero P, Sandberg G, Bennett MJ. 2003. Dissecting *Arabidopsis* lateral root development. *Trends in Plant Science* **8**, 165–171.
- Dolan L, Davies J. 2004. Cell expansion in roots. *Current Opinion in Plant Biology* **7**, 33–39.
- Erickson RO, Sax KB. 1956. Rates of cell division and cell elongation in the growth of the primary root of *Zea mays*. *Proceedings of the American Philosophical Society* **100**, 499–514.
- Ewing B, Hillier L, Wendt MC, Green P. 1998. Base-calling of automated sequencer traces using phred. I. Accuracy assessment. *Genome Research* **3**, 175–185.
- Gowda M, Jantasuriyarat C, Dean RA, Wang GL. 2004. Robust-LongSAGE (RL-SAGE): a substantially improved LongSAGE method for gene discovery and transcriptome analysis. *Plant Physiology* **134**, 890–897.
- Hukin D, Doering-Saad C, Thomas CR, Pritchard J. 2002. Sensitivity of cell hydraulic conductivity to mercury is coincident with symplasmic isolation and expression of plasmalemma aquaporin genes in growing maize roots. *Planta* **215**, 1047–1056.
- Ishikawa H, Evans ML. 1993. The role of the distal elongation zone in the response of maize roots to auxin and gravity. *Plant Physiology* **102**, 1203–1210.
- Ishikawa H, Evans ML. 1995. Specialized zones of development in roots. *Plant Physiology* **109**, 725–727.
- Ishikawa H, Hasenstein KH, Evans ML. 1991. Computer-based video digitizer analysis of surface extension in maize roots; kinetics of growth rate changes during gravitropism. *Planta* **183**, 381–390.
- Klink VP, Alkharouf N, MacDonald M, Matthews B. 2005. Laser capture microdissection (LCM) and expression analyses of *Glycine max* (soybean) syncytium containing root regions formed by the plant pathogen *Heterodera glycines* (soybean cyst nematode). *Plant Molecular Biology* **59**, 965–979.
- Li J, Yang H, Peer WA, Richter G, Blakeslee J, et al. 2005. *Arabidopsis* H⁺-PPase AVP1 regulates auxin-mediated organ development. *Science* **310**, 60–61.
- Liang BM, Sharp RE, Baskin TI. 1997. Regulation of growth anisotropy in well-watered and water-stressed maize roots. I. Spatial distribution of longitudinal, radial, and tangential expansion rates. *Plant Physiology* **115**, 101–111.
- Loudet O, Gaudon V, Trubuil A, Daniel-Vedele F. 2005. Quantitative trait loci controlling root growth and architecture in *Arabidopsis thaliana* confirmed by heterogeneous inbred family. *Theoretical and Applied Genetics* **110**, 742–753.
- Macleod RD. 1991. The root apical meristem and its margins. In: Waisel Y, Eshel A, Kafkafi U, eds. *Plant roots: the hidden half*. New York: Marcel Dekker, 75–101.
- Malamy E. 2005. Intrinsic and environmental response pathways that regulate root system architecture. *Plant, Cell and Environment* **28**, 67–77.
- Muday G, Haworth P. 1994. Tomato root growth, gravitropism, and lateral development. *Plant Physiology and Biochemistry* **32**, 193–203.
- Nakazono M, Qiu F, Borsuk LA, Schnable PS. 2003. Laser-capture microdissection, a tool for the global analysis of gene expression in specific plant cell types: identification of genes expressed differentially in epidermal cells or vascular tissues of maize. *The Plant Cell* **15**, 583–596.
- Noh B, Murphy AS, Spalding EP. 2001. Multidrug resistance-like genes of *Arabidopsis* required for auxin transport and auxin-mediated development. *The Plant Cell* **13**, 2441–2454.
- O'Toole JC, Bland WL. 1987. Genotypic variation in crop plant root systems. *Advances in Agronomy* **41**, 91–145.
- Padmanaban S, Lin X, Perera I, Kawamura Y, Sze H. 2004. Differential expression of vacuolar H⁺-ATPase subunit c genes in tissues active in membrane trafficking and their roles in plant growth as revealed by RNAi. *Plant Physiology* **134**, 1514–1526.
- Pawlowski K, Kunze R, De Vries S, Bisseling T. 1997. Isolation of total, poly(A) and polysomal RNA from plant tissues. In: *Plant molecular biology manual*. 2nd edn. Dordrecht: Kluwer Academic Publishers, 1–13.
- Poroyko V, Hejlek LG, Spollen WG, Springer GK, Nguyen HT, Sharp RE, Bohnert HJ. 2005. The maize root transcriptome by serial analysis of gene expression. *Plant Physiology* **138**, 1700–1710.
- Rashotte AM, Brady SR, Reed RC, Ante SJ, Muday GK. 2000. Basipetal auxin transport is required for gravitropism in roots of *Arabidopsis*. *Plant Physiology* **122**, 481–490.
- Redinbaugh MG, Sabre M, Scandalios JG. 1990. The distribution of catalase activity, isozyme protein, and transcript in the tissues of the developing maize seedling. *Plant Physiology* **92**, 375–380.
- Scheres B, Heidstra R. 1999. Digging out roots: pattern formation, cell division, and morphogenesis in plants. *Current Topics in Developmental Biology* **45**, 207–247.

- Schiefelbein J.** 2003. Cell-fate specification in the epidermis: a common patterning mechanism in the root and shoot. *Current Opinion in Plant Biology* **6**, 74–78.
- Sessions A, Yanofsky MF, Weigel D.** 2000. Cell–cell signaling and movement by the floral transcription factors LEAFY and APE-TALA1. *Science* **289**, 779–782.
- Sharp RE.** 2002. Interaction with ethylene: changing views on the role of abscisic acid in root and shoot growth responses to water stress. *Plant, Cell and Environment* **25**, 211–222.
- Sharp RE, Silk WK, Hsiao TC.** 1988. Growth of the maize primary root at low water potentials. I. Spatial distribution of expansive growth. *Plant Physiology* **87**, 50–57.
- Sharp RE, Poroyko V, Hejlek LG, Spollen WG, Springer GK, Bohnert HJ, Nguyen HT.** 2004. Root growth maintenance during water deficits: physiology to functional genomics. *Journal of Experimental Botany* **55**, 2343–2351.
- Soares B, De Fatima Bonaldo M.** 1997. Constructing and screening normalized cDNA libraries. In: Green ED, Birren B, Klaphols S, Myers RM, Hier P, eds. *Genome analysis: a laboratory manual*, Vol. 2. Cold Spring Harbor, NY: Cold Spring Harbor Laboratory Press. 49–157.
- Spollen WG, LeNoble ME, Samuels TD, Bernstein N, Sharp RE.** 2000. Abscisic acid accumulation maintains maize primary root elongation at low water potentials by restricting ethylene production. *Plant Physiology* **122**, 967–976.
- Tatusov RL, Natale DA, Garkavtsev IV, et al.** 2001. The COG database: new developments in phylogenetic classification of proteins from complete genomes. *Nucleic Acids Research* **29**, 22–28.
- Woll K, Borsuk LA, Stransky H, Nettleton D, Schnable PS, Hochholdinger F.** 2005. Isolation, characterization, and pericycle-specific transcriptome analyses of the novel maize lateral and seminal root initiation mutant *rum1*. *Plant Physiology* **139**, 1255–1267.
- Wu Y, Thorne ET, Sharp RE, Cosgrove DJ.** 2001. Modifications of expansin transcript levels in the maize primary root at low water potentials. *Plant Physiology* **126**, 1471–1479.
- Zhu J, Chen S, Alvarez S, Asirvatham VS, Schachtman DP, Wu Y, Sharp RE.** 2006. Cell wall proteome in the maize primary root elongation zone. I. Extraction and identification of water-soluble and lightly ionically bound proteins. *Plant Physiology* **140**, 311–325.